Arabian Journal of Chemistry (2013) 6, 87–92

King Saud University

Arabian Journal of Chemistry

www.ksu.edu.sa
www.sciencedirect.com

ORIGINAL ARTICLE

Pitting of Al and Al–Si alloys in KSCN solutions and the effect of light

Mohammed A. Amin *

Department of Chemistry, Faculty of Science, Ain Shams University, 11566 Abbassia, Cairo, Egypt
Materials and Corrosion Lab (MCL), Department of Chemistry, Faculty of Science, Taif University, 888 Hawiya, KSA

Received 31 August 2010; accepted 24 September 2010
Available online 2 October 2010

KEYWORDS

Pitting corrosion;
Photo-inhibition;
Al;
Al-Si alloys;
KSCN solutions

Abstract The pitting corrosion susceptibility of pure Al and three Al-Si alloys, namely (Al-6%Si), (Al-12%Si) and (Al-18%Si) has been studied in 0.04 M KSCN solution. Measurements were carried out under the effect of various experimental conditions using cyclic polarization, potentiostatic and galvanostatic techniques. In all cases, the potentiodynamic anodic polarization curves do not exhibit active dissolution region due to spontaneous passivation. The passivity is due to the presence of a thin film of Al_2O_3 on the anode surface. The passive region is followed by pitting corrosion, at a certain critical potential, pitting potential (E_{pit}), as a result of breakdown of the passive film by SCN^- anions. Cyclic polarization measurements allowed the determination of the pitting corrosion parameters, namely the pitting potential and the repassivation potential (E_{rp}). Alloyed Si decreased the passive current (j_{pass}) and shifted both E_{pit} and E_{rp} towards more positive values. Thus alloyed Si suppressed pitting attack. The effect of illumination on passivity and the initiation of pitting corrosion on Al in KSCN solutions was also studied. It is observed that illumination of Al leads to an increase in its pitting corrosion resistance-apparent from j_{pass}, E_{pit}, and E_{rp} measurements in aggressive KSCN solutions.

1. Introduction

The breakdown of passive films that form on metals and alloys and the initiation and propagation of localized corrosion are major concerns in corrosion engineering and are of great fundamental interest in electrochemistry. Various attempts, ranging from the addition of alloying elements to the base material (Amin et al., 2008; Wendt et al., 1994; Shaw et al., 1991; Sedriks, 1979; Natishan et al., 1988; Abd El Rehim et al., 2002) to the addition of inhibitor-containing solutions to the environment (Ohi et al., 1994; Abd El Rehim et al., 2004), have been made in an effort to enhance the passivity of metals and alloys.

* Address: Department of Chemistry, Faculty of Science, Ain Shams University, 11566 Abbassia, Cairo, Egypt. Tel./fax: +20 222509331.
E-mail address: maaismail@yahoo.com

Peer-review under responsibility of King Saud University.
doi:10.1016/j.arabjc.2010.09.022

Production and hosting by Elsevier

Recently, it has been shown that inhibition of localized corrosion can be achieved by illuminating immersed electrodes with UV/visible photons.

The first observation of this kind was reported for polycrystalline nickel in chloride-containing solutions on illuminating with incident white light (Lenhart et al., 1987). More recently, an anodic shift in the breakdown potential of type 304SS in chloride solutions was found in the presence of uv light (Macdonald et al., 1996), while stronger photoinhibition effects were observed for pure iron (Schmuki et al., 1994; Schmuki and Bohni, 1995) under high intensity UV irradiation. Although it was reported, in some earlier studies, that the rate of corrosion of mild steel in citrate- and sulphate-containing solutions increased on illuminating with white light (Bastidas and Scantlebury, 1985; Bastidas and Scantlebury, 1986), these more recent studies suggest that illumination with high energy photons leads to a modification of the passive film that results in an increased resistance to the onset of pitting attack.

It is the aim of this study to examine pitting events on Al and three selected Al-xSi (x = 6, 12 and 18%) alloys in KSCN solutions, based on cyclic polarization, potentiostatic j/t and galvanostatic E/t measurements. The effect of the alloyed Si on the stability of the passive film towards the aggressive attack of SCN^- anions is discussed. It was also the purpose of the present work to study the effect of light on the pitting events on Al surface in aggressive KSCN solutions.

2. Experimental

2.1. Solutions

The electrolyte employed in this study was potassium thiocyanate, KSCN, (the pitting corrosion agent). This electrolyte was purchased from Merck (Darmstadt, Germany). The electrolyte was prepared using analytical grade reagents (Merck) and triply distilled water. Potassium thiocyanate was dissolved in the triply distilled water at a concentration of 0.04 M. The solution temperature was adjusted to the required values (±1 °C), using water thermostat.

2.2. Electrodes and apparatus

Four working electrodes were used in this work; very pure Al rod (99.99 % Koch Light Laboratories, Colnbrook Buckes, UK) and three (Al-xSi) alloys; x = 6, 12 and 18%. For electrochemical measurements, the investigated materials were cut as cylindrical rods, welded with Cu-wire for electrical connection and mounted in glass tubes of appropriate diameter using Araldite to offer an active flat disc-shaped surface of (0.50 cm^2) geometric area, to contact the test solution. Prior to each experiment, the working electrodes were mechanically polished with aluminum powders of different grain sizes down to 0.05 μm, using waters lubricant, and were then repeatedly rinsed with water, dried, and then etched in a 0.10 M NaOH solution for 30 s. The etched electrode was rinsed with deionized water rapidly, followed by immediate rinsing with absolute ethanol. The aim of the NaOH etching method is to produce a fresh and active (oxide-free) electrode surface as much as possible.

The electrochemical set-up consisted of a classical three electrode arrangement, in a transparent polystyrene cell, with a Pt counter electrode and a saturated calomel reference electrode. The SCE was connected via a Luggin capillary, the tip of which was very close to the surface of the working electrode to minimize the IR drop. All potentials given in this paper are referred to this reference electrode. Electrochemical measurements were performed using An Autolab Potentiostat/Galvanostat (PGSTAT30) connected with a personal computer with GPES and FRA (ver. 4.9) software provided by Autolab. The stabilization period prior to collecting data was 12 h.

Cyclic polarization measurements were carried out by sweeping linearly the potential from the starting potential, −2000 mV (SCE), into the positive direction at a scan rate of 0.50 mV s^{-1} till the ending potential, 2000 mV (SCE), and then reversed with the same scan rate till forming a well-defined hysteresis loop. The potentiostatic j/t transient measurements were carried out after a two step procedure, namely: the working electrode was first held at the starting potential for 60 s to attain a reproducible electroreduced electrode surface. Then the electrode was held at constant anodic step potential ($E_{s.a}$) where the anodic current was recorded with time. In galvanostatic measurements, the potential is monitored as a function of time at an anodic current density of 60 μA cm^{-2} to establish a E/t curve for the tested Al samples in 0.04 M KSCN solution. The stabilization period prior to collecting data was 12 h. The open circuit potential of the working electrode was measured as a function of time during this stabilization time. This time was quite sufficient to reach a quasi-stationary value for the open circuit potential.

The working electrode was illuminated through the bottom of the cell with a 250 W tungsten-halogen lamp fed with a variator. A relative intensity scale was established by measuring the photocurrent in a silicon photodiode as a function of the variator setting. In the following, the relative intensities represent the ratio of the photocurrent obtained on the photodiode relative to that when the lamp is fed with its nominal voltage. The latter conditions (100% relative intensity) correspond to a useful photon flux on the order of 10^{17} s^{-1} cm^{-2} (Abdel-Samad et al., 2004). In illumination experiments, the electrodes were illuminated continuously throughout the potential scan. In current–time studies and incubation time measurements, the electrode was initially polarized at E_{corr}, for a 15 min period, and then stepped to an appropriate point where passivity could be observed for the non-illuminated specimens, and the current transients were recorded as a function of time.

3. Results and discussion

3.1. Cyclic polarization plots (estimation of the pitting corrosion parameters)

In order to evaluate the pitting corrosion process of the tested Al samples in KSCN solutions, pitting potentials and other pitting corrosion parameters were estimated from cyclic potentiodynamic curves as a function of sample composition (Fig. 1). These samples in this aggressive medium show a cathodic region (exhibiting Tafel behavior), a free corrosion potential (E_{corr}), an active–passive transition, a passive region and the pitting potential (E_{pit}) indicated by a permanent rise in current in the passive region. At E_{pit}, the aggressive SCN^- anions displace the adsorbed passivating species at some locations and accelerate local anodic dissolution. This mechanism is accelerated when SCN^- concentration increases (Amin

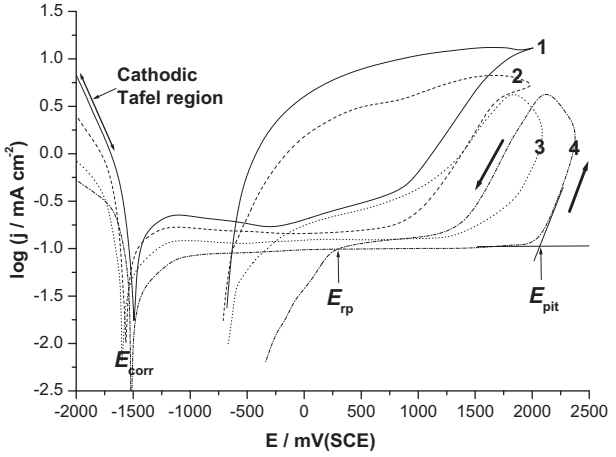

Figure 1 Cyclic polarization plots recorded for Al and its three selected Al–Si alloys in 0.04 M KSCN solution at a scan rate of 0.50 mV s^{-1} at 25 °C. (1) Al; (2) Al–6%Si alloy; (3) Al–12% Si alloy; (4) Al–18% Si alloy.

et al., 2009). Pitting growth occurs as a result of an increase in SCN^- concentration resulting from its migration inside pits and hydrolysis of Al^{3+} ions, since the high acidity required for pitting corrosion site growth must be achieved by hydrolysis of Al^{3+} ions inside pits; see more details in our previous study (Amin et al., 2008; Amin et al., 2009).

The current rise continues even after scan reversal. A current hysteresis loop, characteristic of localized corrosion phenomena, appears. The obtained hysteresis loop allows the repassivation (nucleation) potentials, E_{rp} (E_n) to be determined (Szklarska-Smialowska, 1986). When the critical repassivation or nucleation potential $E_{rp} = E_n$ is reached, the anodic current decreases rapidly. Repassivation potentials correspond to the potential values below which no pitting occurs and above which pit nucleation begins (Amin et al., 2009). Once the cyclic polarization plot is established, pitting potentials, repassivation potentials, nucleation potentials as well as passivation current density (j_{pass}) were calculated as characteristic parameters for defining the behavior of a material in a corrosive medium.

The existence of a hysteresis loop in a cyclic potentiodynamic polarization curve indicates a delay in repassivation of an existing pit when the potential is scanned towards negative direction. The larger the hysteresis loop, the more difficult it becomes to repassivate the pit (Szklarska-Smialowska, 1986). It is obvious that the passivation current diminishes with the alloyed Si content of the sample. At the same time, both E_{pit} and E_{rp} shifted towards more positive values. These results indicate that alloyed Si improves the pitting corrosion resistance of Al to an extent depending on its content in the sample.

The role played by Si in enhancing the pitting corrosion resistance of Al in these solutions may be explained on the basis that any localized dissolution will preferentially dissolve Al and leave the surface enriched in unreactive Si atoms. Enrichment of alloy surface in unreactive Si atoms during dissolution blocks the active sites available for Al dissolution. At this stage, dissolution is retarded and pitting ceases. In order for pitting to recommence, the potential must be raised even higher [to $(E_{pit})_{alloy}$] to activate dissolution at the less favourable sites. As the Si content is increased, Si atoms will appear with greater frequency. Therefore, dissolution processes will be retarded until increasingly higher potentials are reached. Therefore, $(E_{pit})_{alloy}$ must increase with Si content, as shown in the insert of Fig. 1.

Other research workers attributed the high corrosion resistance of Al-Si alloys to the incorporation of Si atoms in the Al_2O_3 passive film (Wood and Brock, 1966). This incorporation repairs the film defects and precludes significant dissolution of the oxide film (Strehblow and Doherty, 1978). This makes it more difficult for the aggressive SCN^- anions to migrate through the oxide film. Si would as a result increase the difficulty of soluble film formation required for film rupture to occur (Foley, 1986). Si may also slow down the rate of metal dissolution by reducing the amount of free metal ions in the pit solution resulting in a decrease in diffusion of SCN^- anions into the pit and in diffusion of metal cations out of the pit (Bohni, 1987). It is also probable that the presence of Si in Al assists the rapid repassivation of the bare metal so that further metal dissolution and, therefore, pit formation is prevented.

3.2. Transient techniques

3.2.1. Potentiostatic *j*/*t* measurements

Fig. 2 illustrates potentiostatic current transients recorded for Al and its three Al–Si alloys subjected to a constant step anodic potential, $E_{s,a}$, of 1600 mV (SCE) in 0.04 M KSCN solution at 25° C. In Fig. 2, it can be seen that the pitting process is categorized into the three stages, i.e. the first passivation stage, the second pit formation and growth stage and the final steady-state stage. The anodic current density of the first stage descended abruptly with time and then reached a current minimum at a certain incubation time, t_1.

The fall of current density indicates thickening of oxide film on the surface. In the second stage, the value of current density ascended from the moment just after t_1 to another time t_2, which is attributed to passivity breakdown induced by the aggressive attack of SCN^- anions and subsequent formation

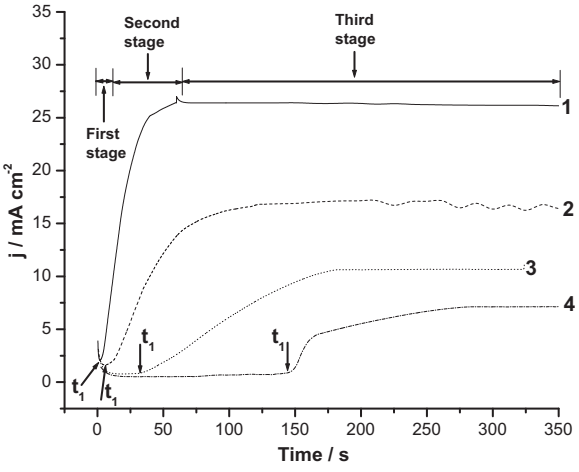

Figure 2 Potentiostatic current-time plots recorded for Al and its three selected Al–Si alloys in 0.04 M KSCN solution at a an applied anodic potential of 1600 mV (SCE) at 25 °C. (1) Al; (2) Al–6% Si alloy; (3) Al–12% Si alloy; (4) Al–18% Si alloy.

and growth of pits (Amin et al., 2009). It is obvious that t_1 and t_2 vary with sample composition, being longer, corresponding to high resistance against pitting, with increasing alloyed Si content in Al samples, see curves 2–4 in Fig. 2.

After pit initiation, see the current rise between t_1 and t_2, it is possible that pitting corrosion products precipitate inside the pits. The corrosion products block up the pits, and therefore, hinder the current flow through the pits. Thus, a steady-state was attained between the metal dissolution and oxide film formation including a blockade by pitting corrosion products in the third stage of current transient after t_2. In the third stage, the increment in current density caused due to the metal dissolution just equals the sum of the decrement in current density due to oxide film formation and the decrement of current density due to the blockade by pitting corrosion products, leading to nearly constant current density.

The current transients presented in Fig. 2 also revealed that there is a growing tendency that the rate of passivation dominates over the rate of oxide dissolution as alloyed Si increased, resulting in the increase in t_1. From the experimental findings that the slope of current transient in the range from t_1 to t_2 is drastically diminished with increasing alloyed Si content, it is deduced that the rate of pit growth suppressed with Si, confirming polarization results.

3.2.2. Galvanostatic E/t measurements

Figs. 3a–d represent the dependence of the anodic potential on time for anodization of Al and Al-6%Si, Al-12%Si and Al-18%Si alloys in 0.04 M KSCN solution at a current density of 60 μA cm^{-2} at 25 °C, respectively. The linear increase in potential at the commencement of anodization accompanies the initial formation and growth of the oxide film. A potential maximum appears at a certain time, assigned as the incubation time, t_i, which is necessary before pit growth to occur. This maximum is thought to correspond, as will be shown, to the pitting potential (E_{pit}). The appearance of which is the correspondence of competition between two processes, namely, further oxide film growth and its breakdown.

The decline in potential following the maximum corresponds to breakdown of passive layer followed by the nucleation and formation of pits as a result of the aggressive attack of SCN^- anions (Amin et al., 2009). After prevalence of the latter reaction at E_{pit}, or in other words, after t_i, the potential drops to a steady value, corresponding to the repassivation potential (E_{rp}). It obvious that the values of E_{rp} obtained from cyclic polarization (Fig. 1) and galvanostatic measurements (Fig. 3) are in good agreements. These findings confirm that the potential maximium observed in the E/t plots corresponds to E_{pit}.

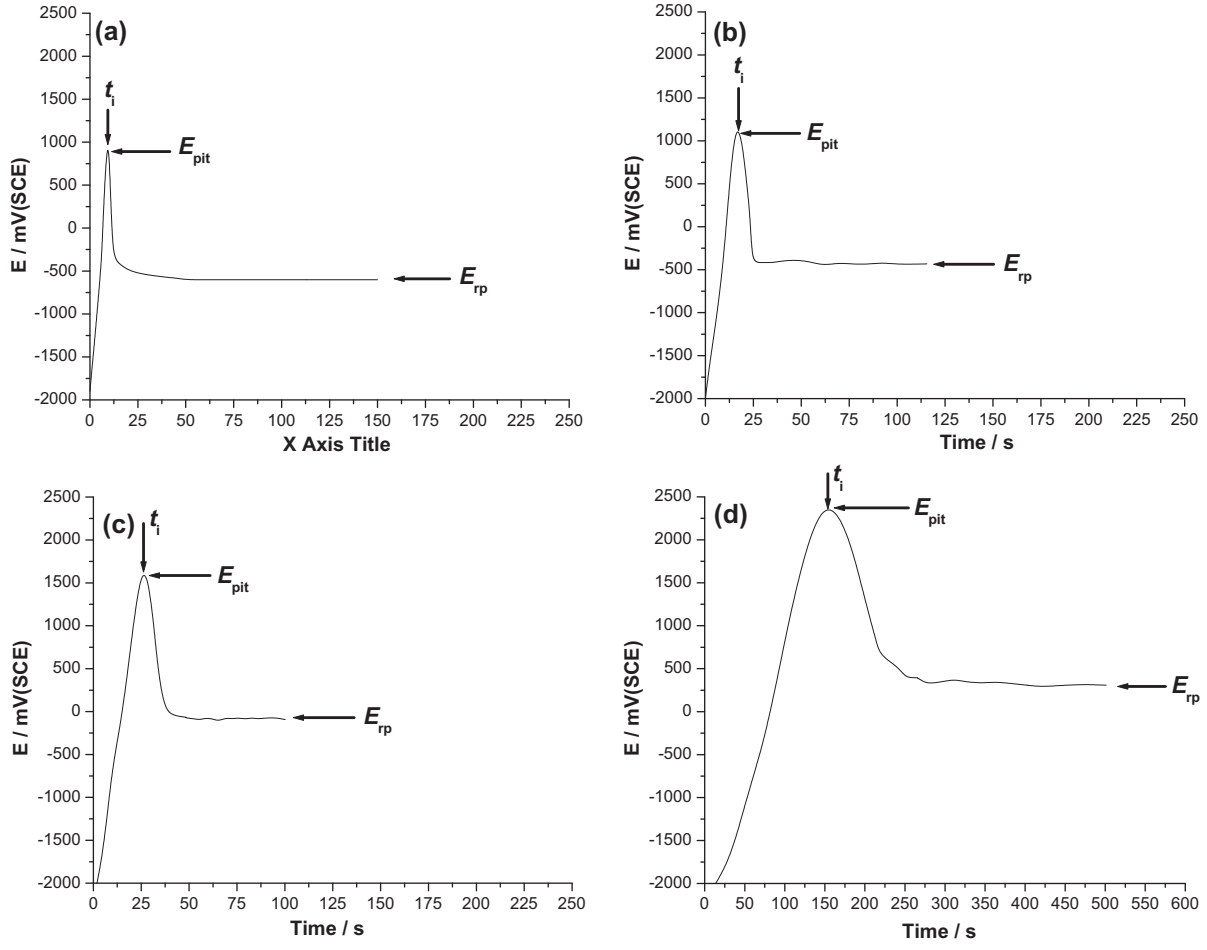

Figure 3 Galvanostatic potential-time plots recorded for (a) Al, (b) Al–6% Si alloy, (c) Al–12% Si alloy, and (d) Al–18% Si alloy in 0.04 M KSCN solution at a an applied anodic current of 60 μA cm^{-2} at 25 °C.

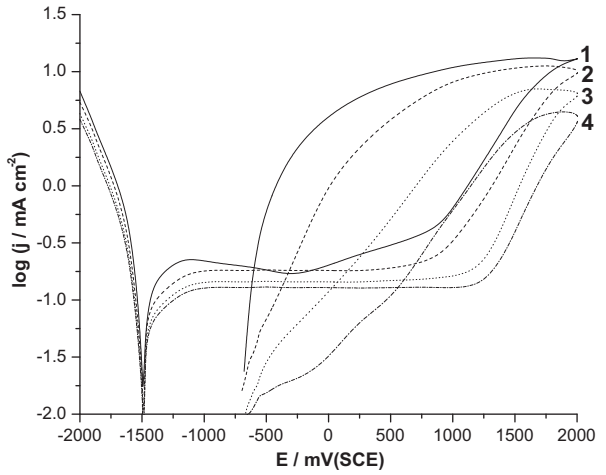

Figure 4 Cyclic polarization curves recorded for Al in 0.04 M KSCN solution as a function of light (arbitrary relative units) intensity at a scan rate of 0.50 mV s^{-1} at 25 °C. (1) Non-illuminated electrode; (2) 20% light; (3) 40% light; (4) 60% light.

It follows from the data of Fig. 3 that the rate of potential increase (i.e., the rate of oxide growth) and the value and location of potential maximum depend on the sample composition. The value of the potential maximum (i.e., E_{pit}) increases and its location shifts towards more positive values (i.e., longer t_i values) when the alloyed Si increases. These findings confirm results of E/j (Fig. 1) and j/t (Fig. 2) measurements that alloyed Si retarded pitting corrosion of Al in KSCN solutions.

3.3. Photo-inhibition of localized corrosion

In this section, the photo-inhibition of pitting on Al in aggressive KSCN solutions and the factors affecting the degree of photo-inhibition are reported. Fig. 4 shows typical cyclic polarization curves recorded for Al in 0.04 M KSCN solution under conditions of illumination (increasing light intensity) and non-illumination. It is evident that an increase in the pitting resistance occurs on illumination of the electrode. Both the pitting and the repassivation potentials are shifted in the noble direction with increase in the light intensity, reflecting an increase in the pitting corrosion resistance. This increased resistance to pitting attack is explained in terms of the semiconducting nature of the passive film. It is proposed that generation of electron-hole pairs leads to a quenching of the electric field strength and consequent modification of the vacancy structure, leading to a decrease in the flux of cation vacancies across the barrier layer.

Comparing Fig. 4 with Fig. 1, it seems that the pitting potentials of the illuminated Al specimens approach those of the (Al-Si) alloys, as measured in the dark. These results indicate perhaps a comparable degree of passivity enhancement between alloying and illumination under these conditions.

Further evidence for photo-inhibition of pitting attack was obtained from j/t measurements, where current-decay transients were monitored as a function of time for illuminated (40% light) and non-illuminated conditions. The obtained plots (not shown here) are very similar to those presented in Fig. 2. A significant increase in the induction periods and a decrease in the rate of pit nucleation were observed for specimens pre-passivated under illumination conditions, indicating that illumination leads to a modification of the passive film that persists even after irradiation is removed.

4. Conclusion

Localized corrosion of Al and Al-6%Si, Al-12%Si and Al-18%Si alloys has been studied in 0.04 M KSCN solutions. Measurements were performed using cyclic polarization and transient (current/time and potential/time) measurements. Obtained results showed that Al and its tested alloys suffered from localized attack in these solutions. Resistance of the tested materials towards localized corrosion increased when the percentage of the alloyed Si increased. Incident photons suppressed the aggressive attack of SCN^- anions. The pitting potential increased with increase in intensity of incident photons. Transient measurements showed that pit initiation and growth decreased in the presence of light.

References

Abd El Rehim, S.S., Hassan, H.H., Amin, M.A., 2002. Corrosion and corrosion inhibition of Al and some alloys in sulphate solutions containing halide ions investigated by an impedance technique. Appl. Surf. Sci. 187, 279.

Abd El Rehim, S.S., Hassan, H.H., Amin, M.A., 2004. Corrosion inhibition study of pure Al and some of its alloys in 1.0 M HCl solution by impedance technique. Corros. Sci. 46, 5.

Abdel-Samad, H.S., Amin, M.A., Chazalviel, J.-N., Ozanam, F., Allongue, P., 2004. Semiconducting photocathodes for the reduction of dioxygen Part I. Characterisation of crystalline and amorphous p-Si. Electrochim. Acta 49, 4577.

Amin, M.A., Abd El Rehim, S.S., Moussa, S.O., Ellithy, A.S., 2008. Pitting corrosion of Al and Al–Cu alloys by ClO_4^- ions in neutral sulphate solutions. Electrochim. Acta 53, 5644.

Amin, M.A., Abd El-Rehim, S.S., El-Sherbini, E.E.F., Mahmoud, S.R., Abbas, M.N., 2009. Pitting corrosion studies on Al and Al–Zn alloys in SCN^- solutions. Electrochim. Acta 54, 4288.

Bastidas, J.M., Scantlebury, J.D., 1985. Photopotentials and the corrosion of mild steel in sodium sulphate solution. Corros. Sci. 25, 377.

Bastidas, J.M., Scantlebury, J.D., 1986. The influence of light on corrosion phenomena: the behaviour of mild steel in citric acid solution. Corros. Sci. 26, 341.

Bohni, H., 1987. Breakdown of passivity and localized corrosion processes. Langmiur 3, 924.

Foley, R.T., 1986. Localized corrosion of aluminium alloys – A Review. Corrosion 42, 277.

Lenhart, S.J., Urquidi-Macdonald, M., Macdonald, D.D., 1987. Photo-inhibition of passivity breakdown on nickel. Electrochim. Acta 32, 1739.

Macdonald, D.D., Sikora, E., Balmas, M.W., Alkire, R.C., 1996. The photo-inhibition of localized corrosion on stainless steel in neutral chloride solution. Corros. Sci. 38, 97.

Natishan, P.M., McCafferty, E., Kubler, G.K., 1988. Surface charge considerations in the pitting of ion-implanted aluminum. J. Electrochem. Soc. 135, 321.

Ohi, M., Nishihara, H., Aramaki, K., 1994. Composite film formation on iron in sulfuric acid by bismuth(III) chloride and benzyl thiocyanate. Corrosion 50, 226.

Schmuki, P., Bohni, H., 1995. Illumination effects on the stability of the passive film on iron. Electrochim. Acta 40, 775.

Schmuki, P., Bohni, H., 1994. Proceedings of the Seoenth International Symposium on Passivity of Metals and Semiconductors. Clausthal-Zellerfeld, Germany, August 21–26.

Sedriks, A.J., 1979. Corrosion of Stainless Steels. The Electrochemical Society, Princeton, NJ.

Shaw, B.A., Shaw, G.D., Fritz, T.L., Rees, B.J., Mdshier, W.C., 1991. Influence of tungsten alloying additions on the passivity of aluminum. J. Electrochem. soc. 138, 3288.

Strehblow, H.H., Doherty, C.J., 1978. Examination of aluminum copper films during anodic oxidation. J. Electrochem. Soc. 125, 30.

Szklarska-Smialowska, Z., 1986. Pitting Corrosion of Metals. NACE, Houston, TX.

Wendt, R.G., Moshier, W.C., Shaw, B., Miller, P., Olson, D.L., 1994. Corrosion-resistant aluminum matrix for graphite-aluminum composites. Corrosion 50, 819.

Wood, G.C., Brock, A.J., 1966. Alternating current resistivity profiles through anodic oxide films on aluminium and its alloys. Nature 209, 773.